Journal Pre-proof

Trimethylacetic anhydride-based derivatization facilitates quantification of histone marks at the MS1 level

Hana Kuchaříková, Pavlína Dobrovolná, Gabriela Lochmanová, Zbyněk Zdráhal

PII: S1535-9476(21)00086-4

DOI: https://doi.org/10.1016/j.mcpro.2021.100114

Reference: MCPRO 100114

To appear in: *Molecular & Cellular Proteomics*

Received Date: 25 November 2020

Revised Date: 11 May 2021

Accepted Date: 8 June 2021

Please cite this article as: Kuchaříková H, Dobrovolná P, Lochmanová G, Zdráhal Z, Trimethylacetic anhydride-based derivatization facilitates quantification of histone marks at the MS1 level, *Molecular & Cellular Proteomics* (2021), doi: https://doi.org/10.1016/j.mcpro.2021.100114.

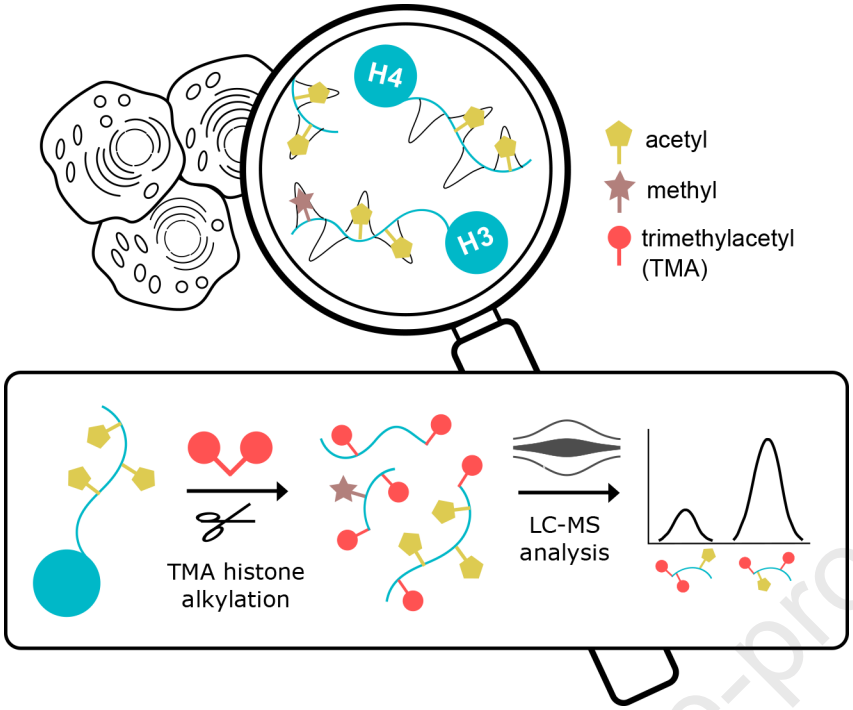

Trimethylacetic anhydride-based derivatization facilitates quantification of histone marks at the MS1 level

Hana Kuchaříková[1,2], Pavlína Dobrovolná[1], Gabriela Lochmanová[1]* and Zbyněk Zdráhal[1,2]*

1 Central European Institute of Technology, Masaryk University, Kamenice 5, 625 00 Brno, Czech Republic

2 Faculty of Science, Masaryk University, Kamenice 5, 625 00 Brno, Czech Republic

*Authors for correspondence:
gabriela.lochmanova@ceitec.muni.cz, zdrahal@sci.muni.cz

Running title: TMA for facilitated MS1-level quantification of histone marks

Abbreviations

Abbreviations - The abbreviations used are:

ACN, acetonitrile; AS, acceptable sequence; ctrl, control samples; DDA, data-dependent acquisition; DIA, data-independent acquisition; EIC, extracted ion chromatogram; enti, entinostat; HDACi, histone deacetylase inhibitor; hPTMs, histone post-translational modifications; MS, mass spectrometry; NHS, N-hydroxysuccinimide ester; PRM, parallel reaction monitoring; Prop, propionic anhydride; TFA, trifluoroacetic acid; TMA, trimethylacetic anhydride; WS, wrong sequence.

KEYWORDS:

Trimethylacetic anhydride, histone post-translational modifications, chemical derivatization, bottom-up proteomics, microwave irradiation

ABSTRACT

Histone post-translational modifications (hPTMs) are epigenetic marks that strongly affect numerous processes, including cell cycling and protein interactions. They have been studied by both antibody- and mass spectrometry-based methods for years, but the analyses are still challenging, mainly due to the diversity of histones and their modifications arising from high contents of reactive amine groups in their amino acid sequences. Here, we introduce use of trimethylacetic anhydride (TMA) as a new reagent for efficient histone derivatization, which is a requirement for bottom-up proteomic hPTM analysis. TMA can derivatize unmodified amine groups of lysine residues and amine groups generated at peptide N-termini by trypsin digestion. The derivatization is facilitated by microwave irradiation, which also reduces incubation times to minutes. We demonstrate that histone derivatization with TMA reliably provides high yields of fully derivatized peptides, and thus is an effective alternative to conventional methods. TMA afforded more than 98 % and 99 % labeling efficiencies for histones H4 and H3, respectively, thereby enabling accurate quantification of peptide forms. Trimethylacetylation substantially improves chromatographic separation of peptide forms, which is essential for direct quantification based on signals extracted from MS1 data. For this purpose, software widely applied by the proteomics community can be used without additional computational development. Thorough comparison with widely applied propionylation highlights the advantages of TMA-based histone derivatization for monitoring hPTMs in biological samples.

INTRODUCTION

In recent years scientists studying diverse biological phenomena have shown increasing interest in characterization of histone post-translational modifications (hPTMs), as they affect overall chromatin structure and form binding sites for effector molecules involved in numerous signaling pathways (1). Thus, together with DNA methylation and action of noncoding RNA, hPTMs are key factors in the regulation of processes that directly involve DNA, including gene expression, DNA repair and replication. Hence, characterization of hPTMs is important for elucidation of fundamental regulatory principles in epigenetics and (*inter alia*) numerous clinical conditions (2). For example, aberrant regulation of hPTMs and recruitment of protein complexes is implicated in human diseases such as various autoimmune and neurological disorders and cancer, as recently reviewed (3–5).

Immunological techniques have been widely used to investigate hPTMs. Currently, chromatin immunoprecipitation coupled with next-generation sequencing (ChIP-Seq) is particularly valuable for mapping genomic regions linked to specific hPTMs. Two decades ago, mass spectrometry (MS) emerged as a sensitive approach for identification and quantification of multiple PTM sites in specific histone variants. For example, using common proteomic pipelines including direct protein digestion with trypsin, the 'zip model' hypothesis was confirmed, showing that acetylation of histone H4 proceeds in the Lys-16 to Lys-5 direction while deacetylation proceeds in the reverse direction (6). By peptide mass fingerprinting using multiple proteases, more than 20 novel modification sites have been revealed that map not only to the globular core but also to C-terminal tail domains of histones (7).

The quantitative capability of MS-based proteomics was clearly demonstrated in a functional analysis of histone deacetylase inhibitor (HDACi) PXD101 using LC-MS/MS. This resulted in quantification of 32 hPTMs at 29 sites from peptide ion intensities, including seven novel PTM sites in histones H2A, H2B, and H4 (8). Introduction of electron transfer dissociation (ETD)/proton transfer reaction (PTR) tandem mass spectrometry enabled characterization of concurrently present PTMs on a single histone tail, thereby facilitating analysis of the roles of combinatorial histone modifications (9). Basically, all major proteomic approaches (top-down, middle-down, and bottom-up) and MS acquisition methods (data-dependent acquisition − DDA, and data-independent acquisition − DIA) have been applied in studies of hPTMs, as recently reviewed (10–12). However, regardless of the method used, histone analysis is still challenging due to the extremely high number of histone variants and complex combinatorial patterns of their modifications. Growing evidence that histone epigenetic marks participate in various physiological and pathological processes has prompted further development of MS-based strategies for hPTM characterization (13–15). These include chemical derivatization of amine groups in histone sequences as a useful strategy for preparing samples for bottom-up LC-MS/MS analysis (16). A two-step derivatization process is usually applied, starting with NH_2-labeling of the protein sequences to obtain longer and more hydrophobic Arg-C-type peptides after trypsin digestion, followed by labeling of newly released NH_2-groups at peptide N-termini to increase the peptides' hydrophobicity and thus their chromatographic retention. Although various chemical agents (and conditions) for labeling have been tested, none have met all the requirements for appropriate and straightforward quantification of isobaric peptides at the MS1 level (11, 17, 18). For instance, use of propionic anhydride (Prop), the most well-established labeling agent for histones, does not enable separation of positional isomers of mono-, di-, and tri-

acetylated peptides of H4 N-termini, or certain di-acetylated peptides of histone H3 on commonly used reversed stationary phases. In addition, there is a tendency for so-called over-propionylation to occur, i.e., side reactions at hydroxyl groups of serine, threonine and tyrosine (17).

In the study presented here, we established a procedure for microwave-assisted labeling of histones prior to bottom-up LC-MS/MS analysis involving use of trimethylacetic anhydride (TMA; also known as pivalic anhydride) for lysine derivatization. This provided substantial advantages for histone quantification using MS1-level spectral information. Microwave irradiation enabled stepwise labeling of histone proteins and peptides, affording high derivatization efficiency. Here, we demonstrate the efficiency of TMA derivatization, chromatographic features of derivatized isobaric peptide forms, and variations in the mass spectrometric data. The derivatization protocol developed was successfully applied to distinguish hPTM states in human cell cultures treated with a HDACi and controls. For an impartial comparison of the TMA-based procedure we also assessed the performance (using the same parameters) of the widely applied propionylation for labeling the same samples.

EXPERIMENTAL PROCEDURES

Experimental design and statistical rationale – The presented study was designed with the following three aims. First, to establish a protocol for histone labeling using TMA. Second, to evaluate its performance and compare it to a well-established labeling technique (propionylation). Third, to investigate levels of TMA-labeled post-translationally modified histone peptides in cells grown under different conditions. For all measurements, histones extracted from MEC-1 cells were used, and there were five biological replicates (i.e., cultures

in five separate flasks). Portions of each culture were treated with HDACi to alter histone modification status, while others were treated with DMSO and used as control samples. Histone extracts were derivatized with either TMA or Prop. In total, 20 samples were subjected to LC-MS/MS analysis in DDA mode. To determine quantities of peptide forms in co-eluting peaks, five TMA-labeled control samples were analyzed using MS in PRM mode. Raw data were searched in Mascot search engine through Proteome Discoverer 2.2 software with the settings described below; threshold ion score (Mascot search engine) for acceptable peptide identification was 30, fragment match threshold for annotation was set to intensity of 10^4. Identifications of selected histone peptides were manually verified, and quantified based on peak areas derived from the EICs using Skyline software, including identification alignment across the raw files based on retention time and *m/z* values. The significance of between-sample differences (control versus enti-treated, or TMA- versus Prop-labeled) was assessed by t-tests. No outliers were detected in the datasets. Details of the statistical analyses are given below.

The mass spectrometry proteomics data have been deposited to the ProteomeXchange Consortium via the PRIDE (19) partner repository with the dataset identifier PXD019502. The data-independent data set has been deposited in the PanoramaPublic database with the url https://panoramaweb.org/Pi0wHl.url.

Cell cultivation and treatment – The chronic lymphocytic leukemia cell line MEC-1 (DSMZ no.: ACC 497; German Collection of Microorganisms and Cell Cultures GmbH) was grown in Iscove´s Modified Dulbecco‘s Medium (Gibco, Thermo Fisher Scientific, MA, USA) with phenol red, 10% (v/v) fetal bovine serum, 2 mM L-glutamine (Gibco, Thermo Fisher Scientific) and 100 IU penicillin/streptomycin at 37 °C and 5 % CO_2. Confluent cells were incubated with entinostat (enti; MS-275; Cayman Chemicals, USA) dissolved in DMSO, at a

final concentration in the growth medium of 20 µM. Control cells (ctrl) were treated with a corresponding concentration of solvent, i.e., 0.15 % (v/v) DMSO. After 24 h incubation, cells were collected, and histones were extracted. Five replicates of each sample were prepared and analyzed.

Histone extract preparation – Histone extracts were prepared following published procedures (20). Briefly, cells were washed twice in ice cold PBS and incubated in lysis buffer consisting of 80 mM NaCl, 20 mM EDTA (Bio-Rad, California, USA), 1% Triton X-100 (Carl Roth, Germany), 45 mM sodium butyrate and 0.1 mM PMSF (Thermo Fisher Scientific) on ice for 20 min and centrifuged at 2000 g for 8 min. Each resulting pellet was resuspended in 900 µL of ice-cold H_2SO_4 (Penta, Czech Republic) and incubated at 4 °C for 2 h. Supernatant cleared by centrifugation at 16000 g and 4 °C for 8 min was diluted with 900 µL of 50% ice-cold trichloroacetic acid and incubated with shaking at 0 °C for 30 min. The resulting precipitate was harvested by centrifugation at 5000 g at 4 °C for 30 min, washed with 50 mM HCl (Penta) in acetone and twice with acetone, then dried at RT. The prepared histone extract was dissolved in water and the protein concentration of the solution was determined with the Bradford Assay (using a Bio-Rad kit).

Histone derivatization – Portions (12 µg) of histone extract were diluted to a final concentration of 1 $\mu g.\mu L^{-1}$ with 50% (v/v) acetonitrile (ACN; Honeywell, USA). The pH was adjusted to 8 with NH_4OH and 3 µL of derivatization reagent consisting of trimethylacetic anhydride (Sigma- Aldrich (MO, USA) and ACN in a 1:3 (v/v) ratio was added to each sample. The samples were incubated for 5 h at RT with shaking, followed by repeated derivatization step including 16 h incubation, and then subjected to two rounds of microwave-assisted derivatization, as follows. Each sample was reduced in volume to approximately 5 µL in a microtube placed in a Savant SPD121P concentrator (Thermo Fisher Scientific), then diluted

with 50% (v/v) ACN to a final volume of 12 µL. The microtube was capped and placed in a glass beaker that was covered with another glass beaker during incubation in a microwave oven for the first round of microwave-assisted derivatization. This consisted of three sub cycles with the following steps: adjustment of the sample's pH to 8 with NH_4OH, addition of 3 µL of derivatization reagent, and two one-minute incubations in the microwave oven at 350 W with a short centrifugation between them. The sample was then concentrated, and the second round of microwave-assisted derivatization was carried out with the same protocol. The resulting labeled protein sample was concentrated to 5 µL, and 0.3 µg of trypsin (Sequencing grade modified, Promega Corporation, WI, USA) in 40 µL of 100 mM ammonium bicarbonate (ABC) was added. After 4 h incubation at 37 °C, another aliquot of 0.3 µg of trypsin was added and the sample was incubated for a further 12 h at 37 °C. The generated peptides were then subjected to a round of microwave-assisted derivatization at N-termini using the protocol described above, then the sample volume was reduced, 50% (v/v) ACN was added to a final volume of 24 µL and another round of microwave-assisted derivatization was carried out with the same protocol. Labeled peptides were dried in a vacuum concentrator overnight. To ensure quantitative recovery of peptides, 60 µL of 50% ACN was added to each sample, followed by vacuum concentration to 15 µL. The sample was diluted with 100 µL of 0.1% trifluoroacetic acid (TFA) and desalted using a HyperSep SpinTip C18 (Thermo Fisher Scientific) following the manufacturer's instructions. Peptides were sequentially eluted with 20 µL of 0.1% TFA in 50% ACN and 2x 20 µL of 0.1% TFA in 75% ACN. Pooled eluates were transferred to a LC vial. Before LC-MS/MS, TFA was evaporated in a vacuum concentrator and the sample was reconstituted in 0.1% formic acid (Honeywell). A step-by-step derivatization protocol including peptide purification is available in Supplemental Data (section 1.1). Chemical derivatization using Prop was performed

following a previously reported protocol (16) described in Supplemental Data (section 2.1). All chemicals were purchased from Sigma - Aldrich (MO, USA) unless otherwise specified.

LC-MS/MS analysis – Samples of both TMA- and prop-labeled peptides were spiked with iRT peptides (Biognosys, Switzerland) and analyzed using an Ultimate 3000 RSLCnano liquid chromatograph coupled to an Orbitrap Fusion Lumos Tribrid mass spectrometer (Thermo Fisher Scientific). Samples (2 µL) of peptide mixtures were injected, concentrated on an in-house trap column packed with X-Bridge BEH 130 C18 sorbent (100 µm x 30 mm, 3.5 µm particles, Waters, MA, USA), and separated on an Acclaim Pepmap100 C18 analytical column (75 µm x 500 mm, 3 µm particles, Thermo Fisher Scientific). Both columns were tempered at 40 °C. The mobile phases used for the gradient elution consisted of a binary mixture of 0.1% formic acid in water (A) and 0.1% formic acid in 80% acetonitrile (B). Peptides were eluted with a 85 min gradient with a 300 $nL.min^{-1}$ flow rate and content of B rising as follows: 5-25 % (0-20 min), 25-29 % (20-30 min), 29-32 % (30-40 min), 32-38 % (40-55 min), 38-50 % (55-75 min) and 50-85 % (75-85 min), followed by isocratic wash of 85 % B (85-95 min). The outlet of the analytical column was connected to a Digital PicoView 550 ion source equipped with PicoTip SilicaTip emitter (New Objective, MA, USA) and Active Background Ion Reduction Device (ESI Source Solutions, MA, USA).

Mass spectra were acquired in data-dependent mode using 350-2000 *m/z* survey scans at a resolution of 60 000 (at *m/z* 200) with an automatic gain control (AGC) target setting of 4×10^5 and maximum injection time of 54 ms. Precursors with charge states from 2+ to 7+ and intensity above 1×10^4 were subjected to HCD fragmentation with normalized collision energy of 30 %. Once fragmented, precursors were excluded for 60 s before the next fragmentation. Precursors were isolated by quadrupole mass filtration with a 1.6 *m/z* isolation window. Tandem mass spectra were obtained for ions with *m/z* values of at least

110 using 30 000 resolution (at *m/z* 200). Ions were accumulated for a target value of 5×10^4 or 500 ms injection time. The cycle time between master scans was 3 s. PRM data were acquired using survey scans with the same parameters as DDA. Tandem MS analysis was targeted to specific precursors (Supplemental Table S1), which were selected in quadrupole with isolation window 1.6 *m/z*. The normalized HCD fragmentation energy was 30 %. Fragment masses were monitored in the *m/z* range 110-2000 with 30 000 resolution (at *m/z* 200). Ions were accumulated for a target value of 5×10^4 or 200 ms injection time.

Data analysis – Raw data acquired in DDA mode were searched against the modified cRAP contamination database (based on http://www.thegpm.org/crap/, 112 sequences), an in-house histone database (v150710, 114 protein sequences, generated from UniProt), and UniProt KB Human database (v180912, taxon ID: 9606, 21053 sequences) using an in-house Mascot search engine (v2.6.2, Matrix Science, United Kingdom) through Proteome Discoverer software (v2.2.0.388, Thermo Fisher Scientific). The mass error tolerances for precursors were 10 ppm for the cRAP database searches and 7 ppm for the others. Corresponding tolerances of MS/MS fragments were 0.5 and 0.03 Da, respectively. Enzyme specificity was set to semiArg-C with two missed cleavages allowed for all databases. Variable modifications set for individual databases were as follows: cRAP - acetylation (K), deamidation (N, Q), oxidation (M), trimethylacetylation (N-term, K, S, T, Y); Uniprot KB Human - acetylation (protein N-term, K) and trimethylacetylation (N-term, K); in-house histone – the same modifications as for the Human database plus trimethylacetylation (S, T, Y), methylation (K, R), dimethylation (K), trimethylation (K). Search results were refined by applying Percolator with a 1 % false discovery rate threshold to peptide spectrum matches. Identifications of selected peptides were manually inspected, their quantity was determined

and manually validated with Skyline software (v19.1.1.248) based on peak areas in EICs. Settings for database searches of propionylated peptides are described in Supplemental Data (section 2).

Statistical analysis – To compare data acquired for TMA- and Prop-labeled samples in terms of reproducibility, the quantitative value of each peptide was $\log_{10}$-transformed. Means and standard deviations of the abundances of peptides detected and quantified following each derivatization technique were calculated and compared by Mann-Whitney tests.

The relative abundances of specific histone H4 modified peptide forms (Fig. 3C) were calculated following a published approach (21). Briefly, areas of peaks assigned to all the forms were treated as composition. Data acquired from replicate samples were combined using geometric means and closure, then further transformed to calculate average compositions in the samples and hence relative abundances of the peptides (in log2 ratios). The KNIME Analytics Platform using R scripts was used for this analysis.

For quantitative comparison of peptide forms between control and enti-treated samples (Fig. 5-7), $\log_{10}$-transformed values were normalized based on a maximal value of summed peptide peak areas in replicate arrays, the mean and standard deviation were calculated for each peptide form, and the t-test was applied. The fold difference in abundance between control and enti-treated samples was calculated for each peptide form, with the thresholds for statistical significance and fold-change set to $p < 0.01$ and > 1.5, respectively.

The overall acetylation status of enti-treated cells and corresponding controls was compared by calculating the abundance of all peptide forms containing acetyl group(s) relative to the abundance of all non-acetylated peptides. The resulting ratio was log2-transformed for each

replicate separately and the t-test was used to assess the significance of differences in each specific form between control and enti-treated samples.

Development and analytical validation of targeted MS measurements – PRM was used to determine quantities of peptide forms in co-eluting peaks, specifically di-acetylated and tri-acetylated forms of H4G4-R17 peptide. All five biological replicates of control samples labeled with TMA were analyzed. Precursor ions for PRM were selected based on the identifications in previous DDA. Their charge, *m/z* and retention time window were used to create a list of parameters for targeted tandem mass spectrometry analysis (Supplemental Table S1). Quantities of diagnostic fragments for certain peptide forms were determined and manually validated using Skyline software (v19.1.1.248) based on peak areas in EICs (DIA, Tier 3). The quantitative representation of co-eluting isomers was calculated by assuming that the abundance (A) of co-eluting isomers (i, j) is represented by their proportion (R) of the precursor peak area ($\mathrm{P_{PA}}$) in a MS1 EIC: $A_i = R_i \times P_{PA}$. For each isomer, R was calculated as the arithmetic mean of proportions of summed peak areas of isomer-specific y- and b- type fragments (y_s, b_s) (eq 1).

$$Ri = \frac{\frac{\sum y_{si}}{\sum y_{si} + \sum y_{sj}} + \frac{\sum b_{si}}{\sum b_{si} + \sum b_{sj}}}{2} \quad (1)$$

Eq. 1 can be altered to calculate abundances of more co-eluting peptides, if needed. If a precursor of a post-translationally modified histone peptide appeared in more than one charge state, abundances of isomers were calculated separately for each charge state then summed.

RESULTS

Workflow description – The workflow for histone labeling using TMA consists of several sequential derivatization steps at both protein and peptide levels. In pilot experiments we found that TMA labeling efficiency increased as incubation time was prolonged to 16 h. Subsequent inclusion of microwave-assisted incubation enabled efficient amine group derivatization with TMA within minutes. For the final version of the protocol presented here, we exploited the accelerated derivatization of amine groups by microwave irradiation while retaining overnight incubation for the first round of protein-level labeling. A scheme of the complete workflow is shown in Figure 1, and the protocol, including troubleshooting, is presented in detail in the Supplemental Data (section 1). Sample preparation was optimized for 12 μg of histone extract, but obviously the amount of sample may be increased if the ratio between amounts of reagents and histone protein is maintained. Protocol performance (in terms of derivatization efficiency, chromatographic behavior of histone peptides, and relevance for detecting changes in histone modification profiles in real biological samples) was evaluated using mammalian histone extracts. In parallel, the same samples were also labeled with Prop to compare pros and cons of the two derivatization procedures (Supplemental Data, section 2). Five biological replicates were used in all experiments, including TMA- and Prop-labeling.

TMA provided high derivatization efficiency of histones – To assess derivatization efficiency and levels of accompanying unspecific reactions of the TMA labeling-based approach, we characterized histone peptide forms by LC-MS/MS. Selected post-translationally modified peptides of protein N-termini from both H3 and H4 histones were quantified using Skyline software. Evaluated peptide forms were classified into the following five subgroups to rate derivatization efficiency. First: *desired* – peptides cleaved at the C-terminus of arginine

residues with complete labeling of all -NH_2 groups. Second: *under* – peptides cleaved at the C-terminus of arginine with incomplete labeling (at least one -NH_2 group remaining unmodified). Third: *over* – peptides cleaved at the C-terminus of arginine with unspecific labeling of -OH groups of serine (S), threonine (T) or tyrosine (Y), regardless of the degree of -NH_2 labeling. Fourth: *acceptable sequence* (AS) – peptides of various lengths containing the same numbers of lysine residues as corresponding desired peptides, regardless of the degree of labeling. Fifth: *wrong sequence* (WS) – incorrectly cleaved peptides with different numbers of lysine residues from desired peptides (Supplemental Table S2). The abundance of all evaluated peptides was summed, and calculated proportions of the sub-groups show that more than 97 % abundance of peptides of both histones H3 and H4 were in the desired category (Fig. 2A and Supplemental Data, section 1.3). To ensure correct quantification of specific forms, peptides in subgroups 2-4 were assigned to corresponding desired peptides, collectively representing a higher-level category called 'assignable'. The assignable category included more than 99 % and 98 % of the histone H3 and H4 peptides, respectively (Fig. 2B and Supplemental Data, section 1.4), while the remaining WS peptides could not be correctly assigned to desired peptide forms or quantified and were thus called 'unassignable'. The overall efficiency of TMA labeling, in terms of the percentage of assignable peptides, was comparable to results obtained following histone derivatization with Prop (Supplemental Data, section 2.4). However, the proportion of desired histone H3 peptides was higher in TMA-labeled samples (~98 %) than in Prop-labeled samples (~92 %), mainly due to a lower frequency of unspecific labeling in TMA derivatization. The proportions of those undesired histone H3 peptides in the TMA- and Prop-labeled samples were 0.3 % and 7.0 %, respectively. Inter-sample variability of histone mark levels related to

the preparation procedure prior to MS was evaluated using the same datasets. In total, 41 and 29 histone H3 and H4 assignable peptide forms identified in TMA- and Prop-labeled samples were selected for the evaluation. The variance in median values and interquartile ranges of $\log_{10}$-transformed peptide precursor areas across the replicates of TMA-labeled samples were < 1.2 % and < 1.4 %, respectively (Fig. 2C and Supplemental Data, section 1.5), compared to < 3.5 % and < 3.1 % across propionylated samples (Supplemental Data, section 2.4). The difference in mean $\log_{10}$-transformed peptide precursor areas between the two derivatization approaches was not significant ($p = 0.582$), but the standard deviations were significantly higher for Prop-labeled than TMA-labeled samples ($p < 0.001$; Fig. 2D).

Mass spectral characteristics of TMA-labeled histone peptides – Analogously to PTMs, chemical derivatization of amine groups results in production of low-mass signature fragment ions during tandem MS, including fragments corresponding to the derivatization label and natural PTMs at N-terminal lysines of peptides. Such ions can support unambiguous assignment of a given mass spectrum to a specific post-translationally modified peptide form. Inspection of MS/MS spectra of TMA-labeled histones revealed characteristic fragmentation peaks corresponding to masses of lysine immonium (*m/z* 101) and related ions (*m/z* 84 and 112) carrying TMA, including N-terminal lysine fragments carrying TMA together with methylation, dimethylation, and acetylation (Supplemental Data, section 3.1), while no diagnostic peaks of lysine modified with TMA and trimethylation were detected in fragmentation spectra. Apparently, derivatization of monomethylated lysines is rarer when using TMA than in propionylation due to steric effects that block proton substitution.

TMA-labeling affords better chromatographic separation of histone peptides than propionylation – Mammalian histone samples labeled with TMA were compared with those

labeled with Prop in terms of number of identified post-translationally modified histone peptide forms and extracted ion chromatogram (EIC) profiles. The results show that TMA-labeled peptides had higher hydrophobicity and their chromatographic peaks were more evenly distributed across the LC-gradient than their propionylated counterparts (Supplemental Data, section 3.2). Labeling of N-termini by TMA increased retention times by 3-6 min. Each TMA-group increased the difference in retention time between TMA-labeled and Prop-labeled samples. Complete trimethylacetylation of naturally non-modified peptide forms increased retention times by 17-42 min, depending on the number of lysine residues in the amino acid sequence (Supplemental Data, section 3.2). The acquired hydrophobicity remarkably influenced the number of identified and quantified post-translationally modified peptide forms at MS1 level. Peptides selected for evaluation included modified forms of the following histone H3 and H4 N-terminal sequences: K9STGGKAPR17 (H3K9-R17), K18QLATKAAR26 (H3K18-R26), K27SAPATGGVKKPHR40 (H3K27-R40), and G4KGGKGLGKGGAKR17 (H4G4-R17). In total, 24 trimethylacetylated and 19 propionylated peptide forms of histones H3 were identified.

The advantages of TMA labeling were even more apparent for peptide sequences with multiple lysine residues (Fig. 3). Improved separation enabled identification of all 16 modified forms of H4G4-R17, while only 10 forms were identified using propionylation due to missing MS/MS spectra of certain forms in co-eluting peaks. Non-acetylated and tetra-acetylated forms were identified using both derivatization reagents (Fig. 3A). The final numbers of peptides quantified based on MS1 precursor ion intensities reflected the chromatographic behavior of peptides labeled with the two derivatization agents. In both cases, there was some co-elution of positional isomers, but this issue was more problematic following propionylation. For instance, in total 14 precursor peaks of H4G4-R17 peptide in

TMA-labeled samples were quantified, compared to seven in Prop-labeled samples. In particular, all four isomers of the mono-acetylated form were identified and separated in individual peaks, all six di-acetylated isomers were identified in five peaks (as just one pair, K5acK8ac and K5acK12ac, co-eluted), and all four isomers were identified within three peaks (due to co-elution of K5acK8acK16ac and K5acK12acK16ac) in TMA-labeled samples. In contrast, following propionylation only three forms of mono-acetylated peptide were identified in two peaks (K16ac and co-eluting K8ac/K12ac), three di-acetylated forms were identified in two peaks (K5acK12ac and co-eluting K8acK16ac/K12acK16ac), and two identified tri-acetylated isomers co-eluted in a single peak (K5acK8acK12ac and K5acK12acK16ac; Fig. 3B). Clearly, the better chromatographic separation of the peptides after TMA derivatization enabled MS1 quantification of more forms than propionylation (Fig. 3C).

Quantities of some co-eluting forms were determined based on the abundance of isomer-specific MS2 fragments. We obtained high quality MS2 spectra of the precursors within a predefined retention time window by parallel reaction monitoring (PRM). Specific fragments of both y- and b- ion series for each co-eluting form were identified and quantified following the approach described in *Experimental procedures*. Proportions of isomers were calculated from precursor peak areas for both co-eluting trimethylacetylated H4G4-R17 peptide pairs. Di-acetylated K5acK8ac/K5acK12ac and tri-acetylated K5acK8acK16ac/K5acK12acK16ac positional isomers occurred in 1:5 and 1:3 ratios, respectively (Supplemental Table S3). Results of a representative quantitative analysis showing precursor peaks of tri-acetylated positional isomers together with their specific fragments are displayed in Figure 4.

Mass spectra of TMA-labeled samples reflect dynamics of histone modification status – The modification status of histones H3 and H4 was determined in cells treated with a HDACi, using TMA labeling followed by mass spectrometry, to examine the procedure's ability to detect changes in histone modification in biological systems. Entinostat (enti), HDACi with proven effectiveness in MEC-1 cells (20), was added to cultures of these cells at a final concentration of 20 µM, and its effect on histone acetylation status was examined after 24 h (see *Experimental procedures* for details).

A 38% increase in overall acetylation of H3K9-R17 peptide was detected, accompanied by a complex change in combinatorial pattern (Fig. 5). Levels of all histone marks except K14ac- and K9me1K14ac-forms differed significantly between enti-treated samples and controls. The higher acetylation state was accompanied by reduced levels of non-acetylated peptides, including those carrying a single group of me1 (methyl group), me2 or me3 at K9. The most pronounced increase in the global level of H3 peptides (51 %) was in abundance of the fully acetylated H3K18-R26 form, while levels of mono-acetylated peptides were not significantly affected by enti-treatment. The level of global acetylation detected in the H3K27-R40 peptide was also similar in enti-treated and control samples, but detailed investigation revealed a significant increase in the K27ac-form, accompanied by a lower level of the K37ac-form. Moreover, enti-induced acetylation affected the abundance of forms carrying methylations at K27. The level of K27me1K37ac peptide was lower in enti-samples than in control samples while the abundance of the di-methylated counterpart and K27me3-form was significantly higher.

Although acquisition of higher hydrophobicity through TMA-labeling enhanced peptides' retention in most cases, detection of H3A1-R8 peptide remained problematic. Only the non-

modified form of this peptide was identified in TMA-labeled samples and methylated counterparts were lost. More details of this particular modified site can be found in Supplemental Data (section 3.3). In addition to modified forms detected in the N-terminal part of the histone H3 sequence, the following modified sites were detected in its core or C-terminal tail: K56ac (Y54-R63), K79ac, K79me1, K79me2 (E73-R83), and K122ac (V117-R128). No significant difference ($P < 0.05$) in those peptide forms was detected between enti-treated samples and controls (Supplemental Table S4).

However, a substantial (37%) increase in global acetylation of H4G4-R17 was detected (Fig. 6). The biggest quantitative differences between enti-treated and control samples were a more than 30-fold increase in abundance of the tetra-acetylated form and 17-fold decrease in the non-modified form. Further, enti induced more than 3-fold decreases in abundance of all four mono-acetylated isomers. Remarkably lower changes in levels of di-acetylated isomers than in other forms were observed. Except for significant decreases in levels of the peptide acetylated at positions K8 and K12, the abundance of all other di-acetylated forms did not differ or slightly increased. Tri-acetylated isomers with acetylation at K16 position substantially contributed to the hyperacetylation state in enti-treated samples (> 6-fold change), as the K5acK8acK12ac peptide's abundance was 2-fold higher than in control samples. In addition, methylated R3 was identified in a peptide carrying multiple lysine acetylations (K8acK12acK16ac and K5acK8acK12acK16ac) in both control and enti-treated samples.

Enti treatment caused a significant increase in abundance of di-methylated H4K20-R36 peptide accompanied by a decrease in abundance of the non-modified form (Fig. 6 and Supplemental Table S4). In addition to the N-terminal region, lysine acetylations were detected at K31 (D24-R36), K59 (G56-R67), K77 (D68-R78), K79 and K91 (K79-R91) in histone

H4 in TMA-treated samples. Levels of these peptide forms were not significantly affected by enti treatment (Supplemental Table S4).

Although TMA derivatization was primarily optimized for characterization of histones H3 and H4, we checked its potential for detecting differences in PTM status of H2A and H2B between control and enti-treated samples. As the diversity of sequential variants of those histones within the chromatin is quite high, a representative variant of each of them—H2A type 3 (Q7L7L0) and H2B type 1-L (Q99880)—was used for detailed inspection of TMA-labeled post-translationally modified peptides. Besides co-translational acetylation of S1 and methylation of R3, acetylations at positions K5 and K9 (G4-R11), K36 (K36-R42), and K95 (N89-R99) were detected in histone H2A. Importantly, enti treatment induced a significant increase in the level of di-acetylated peptide G4-R11 and reduction in the level of its non-modified counterpart (Fig. 7). For H2B, missing arginine residues in the N-terminal part of the sequence led to formation of long peptides with multiple lysines, e.g., PELAKSAPAPKKGSKKAVTKAQKKDGKKR (P1-R29) which has 11 prospective sites (10 lysines plus the N-terminal amine group) of natural modification or chemical derivatization. Clearly, such long peptides are difficult to characterize using bottom-up approaches due to incomplete y-ion series and high combinatorial patterns of PTM sites. From manual inspection of MS/MS data we were able to confirm the presence of acetylations at positions K5, K11, K12, K15, K16, and K20. However, the data did not enable determination of combinatorial patterns of multiply modified forms and quantification of their abundance.

Histone modification status was also examined in enti-treated and control samples labeled with Prop (Supplemental Data, section 2.5 and Supplemental Table S4). Although higher sequence coverage of histone proteins was obtained using Prop, a smaller number of modified peptide forms was identified and quantified. The overall acetylation trend was

similar to that observed in TMA-treated samples, but detailed quantification of propionylated peptide forms was hindered by frequent presence of co-eluting peaks of isobaric peptides in the MS1-level spectra and missing identification of certain modified sites (e.g., H3K56ac, H3K79ac, H3K122ac, H4K31ac, H4K59ac, H4K77ac, H4K79ac, and H4K91ac). TMA enabled identification of majority most acetylated and methylated forms annotated in the UniProt database or reported in previous studies (7, 8, 22). An overview of histone marks identified in amino acid sequences of histones H3.1, H4, and selected variants of H2A and H2B, including combinatorial patterns of the peptide forms, following TMA and Prop labeling is presented in Supplemental Data (sections 3.4. and 3.5).

DISCUSSION

The altered properties of histone peptides due to derivatization of amine residues substantially affect MS-based quantification of modified forms. In addition to desired and advantageous changes, such as Arg-C-like digestion and improvements in peptide retention on chromatographic columns, chemical derivatization has several adverse effects that should be considered during data evaluation. The accurate quantification of histone marks in biological samples is hindered by unpredictable effects of peptide modifications (both added chemical labels and naturally occurring PTMs) on ionization efficiency (18, 23). However, relative values can be used to compare differences in histone mark levels associated with different biological conditions (24). Alternatively, previously published catalogs of LC-MS response factors, i.e., correction factors determined by normalizing signals of acetylated and methylated synthetic peptides to the abundance of cleaved quantification tags, can be used to facilitate interpretation of histone marks' cellular abundance (23). The possibility that certain natural peptide forms may split into more chromatographic peaks due to side

reactions or incomplete labeling should be also considered. Such drawbacks have been previously reported by several research groups for the widely used derivatization agent propionic anhydride (17, 18, 25, 26). During chemical derivatization of amino moieties, side products can be formed by reaction of acid anhydrides with hydroxyl groups of S, T or Y. Although protocols including hydroxylamine treatment or boiling of propionylated peptides for the reversion of non-specific O-acylation have been established (27), such approaches are not suitable for histone preparation as even natural PTMs are lost during hydrolysis of ester bonds. N-hydroxysuccinimide ester (NHS) has reported potential as an amine-specific alternative to Prop, providing higher than 90% conversion rates of histone peptides (25). However, over-propionylation of certain peptides after NHS labeling has also been described (17). Another disadvantage of propionylation is that increases hydrophobicity less than derivatives obtained using various organic acid anhydrides (18). Moreover, propionylation does not satisfactorily improve chromatographic outcomes with conventionally used reversed stationary phases in terms of separation of positional isomers. Due to the presence of multiple lysines in the histone sequences, more than two isobaric peptides co-elute quite frequently. The identification of peptides in co-eluting peaks is hindered by intensity-based precursor selection in DDA mode. During peak elution, limited numbers of mass spectra can be obtained and not all precursors in a co-eluting peak will yield good fragmentation spectra that enable identification of the peptide forms.

The discrimination of isobaric peptides is a major challenge in quantification of post-translationally modified histone peptides. DIA is currently gaining increasing attention due to the possibility to integrate signals in EICs of both precursor and fragment ions, which reportedly leads to more accurate quantification (28–31). However, this approach relies on a limited number of specific fragment ions in analyses of histone positional isomers.

The development of the procedure presented here was prompted by a need for better separation of specific modified histone peptide forms. In our experiments, evaluation of DDA datasets of TMA- and Prop-labeled histone peptides revealed comparable overall modification status in mammalian cell cultures. However, trimethylacetylation provided substantially better separation of positional isomers, thereby enabling direct quantification of most post-translationally modified peptide forms originating from histones H2A, H3, and H4 from MS1-level EICs using common proteomic software.

However, some particular histone peptides (e.g., hydrophilic methylated H3K4 and long Arg-C-like N-terminal peptides of H2B variants) still pose challenges. For identifying methylated H3K4, Prop-PIC hybrid labeling seems to be the currently preferred method (26, 32–35). This can reportedly shift retention times of mono-, di-, and tri-methylated forms of the T3-R8 peptide by 8-12 min (26). Such increases in hydrophobicity in combination with direct injection for LC and data acquisition based on a mass inclusion list for histone H3 could have substantially contributed to identification of the respective peptides. We presume that proton substitution with TMA at a N-terminal amino acid is probably not sufficient to improve retention of methylated T3-R8 peptides. Thus, further inspection and optimization of particular preparation steps of the presented protocol are needed i.e., purification of peptides on HyperSep SpinTip C18, their retention on trap columns, and identification using targeted data acquisition.

In addition, bottom-up proteomic approaches (with or without chemical derivatization of lysines) has limitations for characterizing PTMs of H2B histones. Due to sparse representation of arginine residues in sequences of H2B variants, multiple PTMs of long Arg-C-like peptides originating from derivatized H2B histones are difficult to localize. For instance, in this study we identified acetylations at six lysine residues of P1-R29 peptide (K5,

K11, K12, K15, K16, and K20), but could not determine their combinatorial pattern due to missing MS/MS fragment ions. On the other hand, trypsin digestion of H2B without derivatization generates multiple N-terminal peptides of different lengths, which also hinders quantitative analysis.

In summary, there is no universally suitable approach for PTM characterization of all core histones and their variants, and the analytical setup must be tailored in accordance with the main experimental objectives. However, the high efficiency and specificity of microwave oven-assisted TMA derivatization, together with its provision of highly reproducible quantitative data, clearly indicate that it is a reliable and effective alternative to established methods for preparing histone samples for bottom-up proteomic analysis. The presented method is ready to use for monitoring alterations in PTM patterns of histone H2A, H3, and H4 in cells, as demonstrated by our experiment with HDACi-treated human cell cultures. Most known acetylation and methylation sites were detected and quantified from MS1-level EICs, including isobaric peptides carrying multiple modifications. Thus, we anticipate that the TMA-based approach will facilitate investigation of epigenetic abnormalities associated with various developmental and pathological conditions, including human diseases.

Data availability

The mass spectrometry proteomics data have been deposited to the ProteomeXchange Consortium via the PRIDE (19) partner repository with the dataset identifier PXD019502. The data-independent data set has been deposited in the PanoramaPublic database and can be accessed via the url https://panoramaweb.org/Pi0wHl.url.

This article contains supplemental data.

Supplemental Data - Detailed derivatization protocol including troubleshooting, protocol for propionic anhydride derivatization, derivatization efficiency data, assignable peptides data, identification parameters of TMA- and Prop-labeled histone peptides (PDF).

Supplemental Table S1 (XLSX) - Precursors for PRM analysis

Supplemental Table S2 (XLSX) - Assigned and quantified peptide sequences

Supplemental Table S3 (XLSX) - Calculation of co-eluting forms' quantities

Supplemental Table S4 (XLSX) - Data used to calculate abundance of histone modifications

CONFLICT OF INTEREST

The authors declare that the research was conducted in the absence of any commercial or financial relationships that could be construed as a potential conflict of interest.

ACKNOWLEDGMENT

This work was supported by the Czech Science Foundation (project No. 19-29701L). CIISB, an Instruct-CZ Centre of the Instruct-ERIC EU consortium, funded by MEYS CR infrastructure project LM2018127, is gratefully acknowledged for financial support of the measurements at the CEITEC Proteomics Core Facility. We thank Prof. Vladimír Šindelář and his colleagues from the Department of Chemistry, Faculty of Science, Masaryk University for proposing potential derivatization agents, including trimethylacetic anhydride.

AUTHOR INFORMATION

Co-corresponding Authors

Gabriela Lochmanová: gabriela.lochmanova@ceitec.muni.cz

Zbyněk Zdráhal: zdrahal@sci.muni.cz

Author Contributions

Hana Kuchaříková: Investigation, Formal analysis, Writing - Original Draft

Pavlína Dobrovolná: Investigation, Formal analysis

Gabriela Lochmanová: Conceptualization, Validation, Writing—Original Draft Preparation

Zbyněk Zdráhal: Conceptualization, Writing - Review & Editing

All authors have approved the final version of the manuscript.

REFERENCES

1. Bowman, G. D.,Poirier, M. G. (2015) Post-Translational Modifications of Histones That Influence Nucleosome Dynamics. *Chemical Reviews* ***115***, 2274–2295. https://doi.org/10.1021/cr500350x.
2. Chen, Z.,Li, S.,Subramaniam, S.,Shyy, J. Y. J.,Chien, S. (2017) Epigenetic Regulation: A New Frontier for Biomedical Engineers. *Annual Review of Biomedical Engineering* ***19***, 195–219. https://doi.org/10.1146/annurev-bioeng-071516-044720.
3. Portela, A.,Esteller, M. (2010) Epigenetic Modifications and Human Disease. *Nature Biotechnology* ***28***, 1057–1068. https://doi.org/10.1038/nbt.1685.
4. Noberini, R.,Sigismondo, G.,Bonaldi, T. (2016) The Contribution of Mass Spectrometry-Based Proteomics to Understanding Epigenetics. *Epigenomics* ***8***, 429–445. https://doi.org/10.2217/epi.15.108.
5. Cheng, Y.,He, C.,Wang, M.,Ma, X.,Mo, F.,Yang, S.,Han, J.,Wei, X. (2019) Targeting Epigenetic Regulators for Cancer Therapy: Mechanisms and Advances in Clinical Trials. *Signal Transduction and Targeted*

Therapy ***4***. https://doi.org/10.1038/s41392-019-0095-0.

6. Zhang, K.,Williams, K. E.,Huang, L.,Yau, P.,Siino, J. S.,Bradbury, E. M.,Jones, P. R.,Minch, M. J.,Burlingame, A. L. (2002) Histone Acetylation and Deacetylation: Identification of Acetylation and Methylation Sites of HeLa Histone H4 by Mass Spectrometry. *Molecular & Cellular Proteomics : MCP* ***1***, 500–508. https://doi.org/10.1074/mcp.M200031-MCP200.

7. Zhang, L.,Eugeni, E. E.,Parthun, M. R.,Freitas, M. A. (2003) Identification of Novel Histone Post-Translational Modifications by Peptide Mass Fingerprinting. *Chromosoma* ***112***, 77–86. https://doi.org/10.1007/s00412-003-0244-6.

8. Beck, H. C.,Nielsen, E. C.,Matthiesen, R.,Jensen, L. H.,Sehested, M.,Finn, P.,Grauslund, M.,Hansen, A. M.,Jensen, O. N. (2006) Quantitative Proteomic Analysis of Post-Translational Modifications of Human Histones. *Molecular and Cellular Proteomics* ***5***, 1314–1325. https://doi.org/10.1074/mcp.M600007-MCP200.

9. Taverna, S. D.,Ueberheide, B. M.,Liu, Y.,Tackett, A. J.,Diaz, R. L.,Shabanowitz, J.,Chait, B. T.,Hunt, D. F.,Allis, C. D. (2007) Long-Distance Combinatorial Linkage between Methylation and Acetylation on Histone H3 N Termini. *Proceedings of the National Academy of Sciences of the United States of America* ***104***, 2086–2091. https://doi.org/10.1073/pnas.0610993104.

10. Toby, T. K.,Fornelli, L.,Kelleher, N. L. (2017) Progress in Top-Down Proteomics and the Analysis of Proteoforms. *Annual Review of Analytical Chemistry* ***9***, 499–519. https://doi.org/10.1146/annurev-anchem-071015-041550.

11. El Kennani, S.,Crespo, M.,Govin, J.,Pflieger, D. (2018) Proteomic Analysis of Histone Variants and Their PTMs: Strategies and Pitfalls. *Proteomes* ***6***, 1–16. https://doi.org/10.3390/proteomes6030029.

12. Sidoli, S.,Garcia, B. A. (2017) Middle-Down Proteomics: A Still Unexploited Resource for Chromatin Biology. *Expert Review of Proteomics* ***14***, 617–626. https://doi.org/10.1080/14789450.2017.1345632.

13. Gargano, A. F. G.,Shaw, J. B.,Zhou, M.,Wilkins, C. S.,Fillmore, T. L.,Moore, R. J.,Somsen, G. W.,Paša-Tolić, L. (2018) Increasing the Separation Capacity of Intact Histone Proteoforms Chromatography Coupling Online Weak Cation Exchange-HILIC to Reversed Phase LC UVPD-HRMS. *Journal of Proteome Research* ***17***, 3791–3800. https://doi.org/10.1021/acs.jproteome.8b00458.

14. Holt, M. V,Wang, T.,Young, N. L. (2019) High-Throughput Quantitative Top-Down Proteomics: Histone H4. *Journal of the American Society for Mass Spectrometry* ***30***, 2548–2560.

https://doi.org/10.1007/s13361-019-02350-z.

15. Janssen, K. A.,Coradin, M.,Lu, C.,Sidoli, S.,Garcia, B. A. (2019) Quantitation of Single and Combinatorial Histone Modifications by Integrated Chromatography of Bottom-up Peptides and Middle-down Polypeptide Tails. *Journal of the American Society for Mass Spectrometry* ***30***, 2449–2459. https://doi.org/10.1007/s13361-019-02303-6.

16. Sidoli, S.,Bhanu, N. V.,Karch, K. R.,Wang, X.,Garcia, B. A. (2016) Complete Workflow for Analysis of Histone Post-Translational Modifications Using Bottom-up Mass Spectrometry: From Histone Extraction to Data Analysis. *Journal of Visualized Experiments* ***2016***, 1–11. https://doi.org/10.3791/54112.

17. Meert, P.,Govaert, E.,Scheerlinck, E.,Dhaenens, M.,Deforce, D. (2015) Pitfalls in Histone Propionylation during Bottom-up Mass Spectrometry Analysis. *Proteomics* ***15***, 2966–2971. https://doi.org/10.1002/pmic.201400569.

18. Sidoli, S.,Yuan, Z. F.,Lin, S.,Karch, K.,Wang, X.,Bhanu, N.,Arnaudo, A. M.,Britton, L. M.,Cao, X. J.,Gonzales-Cope, M.,Han, Y.,Liu, S.,Molden, R. C.,Wein, S.,Afjehi-Sadat, L.,Garcia, B. A. (2015) Drawbacks in the Use of Unconventional Hydrophobic Anhydrides for Histone Derivatization in Bottom-up Proteomics PTM Analysis. *Proteomics* ***15***, 1459–1469. https://doi.org/10.1002/pmic.201400483.

19. Perez-Riverol, Y.,Csordas, A.,Bai, J.,Bernal-Llinares, M.,Hewapathirana, S.,Kundu, D. J.,Inuganti, A.,Griss, J.,Mayer, G.,Eisenacher, M.,Pérez, E.,Uszkoreit, J.,Pfeuffer, J.,Sachsenberg, T.,Yilmaz, Ş.,Tiwary, S.,Cox, J.,Audain, E.,Walzer, M.,Jarnuczak, A. F.,Ternent, T.,Brazma, A.,Vizcaíno, J. A. (2019) The PRIDE Database and Related Tools and Resources in 2019: Improving Support for Quantification Data. *Nucleic Acids Research* ***47***, D442–D450. https://doi.org/10.1093/nar/gky1106.

20. Činčárová, L.,Lochmanová, G.,Nováková, K.,Šultesová, P.,Konečná, H.,Fajkusová, L.,Fajkus, J.,Zdráhal, Z. (2012) A Combined Approach for the Study of Histone Deacetylase Inhibitors. *Molecular BioSystems* ***8***, 2937–2945. https://doi.org/10.1039/c2mb25136a.

21. Lochmanova, G.,Ihnatova, I.,Kucharikova, H.,Brabencova, S.,Zachova, D.,Fajkus, J.,Zdrahal, Z.,Fojtova, M. (2019) Different Modes of Action of Genetic and Chemical Downregulation of Histone Deacetylases with Respect to Plant Development and Histone Modifications. *International Journal of Molecular Sciences* ***20***, 5093. https://doi.org/doi:10.3390/ijms20205093.

22. Filippakopoulos, P.,Picaud, S.,Mangos, M.,Keates, T.,Lambert, J. P.,Barsyte-Lovejoy, D.,Felletar, I.,Volkmer, R.,Müller, S.,Pawson, T.,Gingras, A. C.,Arrowsmith, C. H.,Knapp, S. (2012) Histone Recognition and Large-Scale Structural Analysis of the Human Bromodomain Family. *Cell* ***149***, 214–231. https://doi.org/10.1016/j.cell.2012.02.013.

23. Feller, C.,Forné, I.,Imhof, A.,Becker, P. B. (2015) Global and Specific Responses of the Histone Acetylome to Systematic Perturbation. *Molecular Cell* ***57***, 559–572. https://doi.org/10.1016/j.molcel.2014.12.008.

24. Bártová, E.,Lochmanová, G.,Legartová, S.,Suchánková, J.,Fedr, R.,Krejčí, J.,Zdráhal, Z. (2018) Irradiation by γ-Rays Reduces the Level of H3S10 Phosphorylation and Weakens the G2 Phase-Dependent Interaction between H3S10 Phosphorylation and ГH2AX. *Biochimie* ***154***, 86–98. https://doi.org/10.1016/j.biochi.2018.07.029.

25. Liao, R.,Wu, H.,Deng, H.,Yu, Y.,Hu, M.,Zhai, H.,Yang, P.,Zhou, S.,Yi, W. (2013) Specific and Efficient N-Propionylation of Histones with Propionic Acid N-Hydroxysuccinimide Ester for Histone Marks Characterization by LC-MS. *Analytical Chemistry* ***85***, 2253–2259. https://doi.org/10.1021/ac303171h.

26. Maile, T. M.,Izrael-Tomasevic, A.,Cheung, T.,Guler, G. D.,Tindell, C.,Masselot, A.,Liang, J.,Zhao, F.,Trojer, P.,Classon, M.,Arnott, D. (2015) Mass Spectrometric Quantification of Histone Post-Translational Modifications by a Hybrid Chemical Labeling Method. *Molecular and Cellular Proteomics* ***14***, 1148–1158. https://doi.org/10.1074/mcp.O114.046573.

27. Meert, P.,Dierickx, S.,Govaert, E.,De Clerck, L.,Willems, S.,Dhaenens, M.,Deforce, D. (2016) Tackling Aspecific Side Reactions during Histone Propionylation: The Promise of Reversing Overpropionylation. *Proteomics* ***16***, 1970–1974. https://doi.org/10.1002/pmic.201600045.

28. Marchione, D. M.,Lisby, A.,Viaene, A. N.,Santi, M.,Nasrallah, M. L.,Wang, L. P.,Williams, E. A.,Larque, A. B.,Chebib, I.,Garcia, B. A.,Wojcik, J. B. (2019) Histone H3K27 Dimethyl Loss Is Highly Specific for Malignant Peripheral Nerve Sheath Tumor and Distinguishes True PRC2 Loss from Isolated H3K27 Trimethyl Loss. *Modern Pathology* ***32***, 1434–1446. https://doi.org/10.1038/s41379-019-0287-8.

29. Li, Q. L.,Wang, D. Y.,Ju, L. G.,Yao, J.,Gao, C.,Lei, P. J.,Li, L. Y.,Zhao, X. L.,Wu, M. (2019) The Hyper-Activation of Transcriptional Enhancers in Breast Cancer. *Clinical Epigenetics* ***11***, 1–17. https://doi.org/10.1186/s13148-019-0645-x.

30. Shastrula, P. K.,Lund, P. J.,Garcia, B. A.,Janicki, S. M. (2018) Rpp29 Regulates Histone H3.3 Chromatin

Assembly through Transcriptional Mechanisms. *Journal of Biological Chemistry* ***293***, 12360–12377. https://doi.org/10.1074/jbc.RA118.001845.

31. Sidoli, S.,Lopes, M.,Lund, P. J.,Goldman, N.,Fasolino, M.,Coradin, M.,Kulej, K.,Bhanu, N. V.,Vahedi, G.,Garcia, B. A. (2019) A Mass Spectrometry-Based Assay Using Metabolic Labeling to Rapidly Monitor Chromatin Accessibility of Modified Histone Proteins. *Scientific Reports* ***9***, 1–15. https://doi.org/10.1038/s41598-019-49894-4.

32. Pham, V.,Pitti, R.,Tindell, C. A.,Cheung, T. K.,Masselot, A.,Stephan, J. P.,Guler, G. D.,Wilson, C.,Lill, J.,Arnott, D.,Classon, M. (2020) Proteomic Analyses Identify a Novel Role for EZH2 in the Initiation of Cancer Cell Drug Tolerance. *Journal of Proteome Research* ***19***, 1533–1547. https://doi.org/10.1021/acs.jproteome.9b00773.

33. Restellini, C.,Cuomo, A.,Lupia, M.,Giordano, M.,Bonaldi, T.,Noberini, R. (2019) Alternative Digestion Approaches Improve Histone Modification Mapping by Mass Spectrometry in Clinical Samples. *Proteomics - Clinical Applications* ***13***, 1–7. https://doi.org/10.1002/prca.201700166.

34. Leadem, B. R.,Kagiampakis, I.,Wilson, C.,Cheung, T. K.,Arnott, D.,Trojer, P.,Classon, M.,Easwaran, H.,Baylin, S. B. (2018) A KDM5 Inhibitor Increases Global H3K4 Trimethylation Occupancy and Enhances the Biological Efficacy of 5-Aza-2'-Deoxycytidine. *Cancer Research* ***78***, 1127–1139. https://doi.org/10.1158/0008-5472.CAN-17-1453.

35. Su, Z.,Wang, F.,Lee, J. H.,Stephens, K. E.,Papazyan, R.,Voronina, E.,Krautkramer, K. A.,Raman, A.,Thorpe, J. J.,Boersma, M. D.,Kuznetsov, V. I.,Miller, M. D.,Taverna, S. D.,Phillips, G. N.,Denu, J. M. (2016) Reader Domain Specificity and Lysine Demethylase-4 Family Function. *Nature Communications* ***7***, 1–15. https://doi.org/10.1038/ncomms13387.

Figure captions

FIG. 1. **Histone derivatization with TMA.** *A*, Illustrative scheme of the workflow. *B*, Description of basic steps of the derivatization protocol.

FIG. 2. **Conversion rate and reproducibility of trimethylacetic anhydride derivatization.** *A*, Proportions of histone H3 and H4 peptides in five categories: 1 – *desired* (properly digested and fully derivatized), 2 – *under* (properly digested, but not completely derivatized), 3 – *over* (properly digested and derivatized at S/T/Y residues), 4 – *AS* (acceptable sequences, i.e., peptides of various lengths with the same number of lysine residues as corresponding desired peptides), 5- *WS* (wrong sequences, i.e., peptides with different numbers of lysine residue from desired peptides). *B*, Proportions of assignable peptides, i.e., peptides enabling correct quantification. *C*, Distribution of $\log_{10}$- transformed precursor EIC peak areas of assignable peptides showing the reproducibility of histone derivatization across the replicates. The box-plots show extremes, interquartile ranges and medians (N = 41). *D*, Comparison of means and standard deviations of histone H3 and H4 peptide forms' abundances in the TMA- and Prop- labeled samples. The box-plots show extremes, interquartile ranges and medians (N = 41 and 29 for TMA and Prop, respectively); p-values were obtained from comparison of means and standard deviations by Mann-Whitney tests.

FIG. 3. **Comparison of TMA- and Prop- derivatized H4G4-R17 peptide forms.** *A*, Overview of modified histone-peptide forms identified by LC-MS/MS. Peptide forms separated, using each derivatization agent, into individual peaks (✓), co-eluting forms, and unidentified forms (x) are indicated. *B*, Elution profiles of positional isomers of mono-, di-, and tri-acetylated peptides. *C*, Representation of quantified forms.

FIG. 4. **Specific fragment ions of co-eluting tri-acetylated forms of H4G4-R17 peptide after TMA derivatization.** *A*, Representative co-eluting precursor peak of K5acK8acK16ac and K5acK12acK16ac forms and peaks of their y- and b- specific fragments obtained in LC-MS/MS PRM analysis. *B*, Fragments of y- and b- ion series for K5acK8acK16ac and K5acK12acK16ac peptide forms with corresponding *m/z* values. Specific fragments for each form are marked in bold.

FIG. 5. **Modification dynamics of histone H3 N-termini in enti-treated and control (ctrl) samples.** Five replicates of each group were subjected to LC-MS/MS analysis in DDA mode; mean values and SDs are

presented. Relative proportions of non-acetylated and acetylated peptide forms (left), and the abundance of selected modified peptide forms after log_{10} transformation and normalization (right). Asterisks (**) indicate significant differences (<0.01) between the groups, according to t-tests, with > 1.5 fold-changes (Supplemental Table S4).

FIG. 6. **Modification dynamics of histone H4 N-termini in enti-treated and control (ctrl) samples.** Five replicates of each group were subjected to LC-MS/MS analysis in DDA mode; mean values and SDs are presented. Relative proportions of non-acetylated to acetylated peptide forms of H4G4-R17 peptide (left), and the abundance of selected modified peptide forms after log_{10} transformation and normalization (right). Significant changes in methylation status were found in the H4K20-R36 peptide. Asterisks (**) indicate significant differences (<0.01) between the groups, according to t-tests, with > 1.5 fold-changes (Supplemental Table S4). Co-eluting H4G4-R17 peptide forms (K5acK8ac/K5acK12ac and K5acK8acK16ac/K5acK12acK16ac) can be distinguished and quantified based on PRM data as described in *Experimental procedures*.

FIG. 7. Modification dynamics of histone H2A.3 N-termini in enti-treated and control (ctrl) samples. Five replicates of each group were subjected to LC-MS/MS analysis in DDA mode; mean values and SDs are presented. Relative proportions of non-acetylated to acetylated peptide forms (left), and the abundance of selected modified peptide forms after log10 transformation and normalization (right). Asterisks (**) indicate significant differences (<0.01) between the groups, according to t-tests, with > 1.5 fold-changes (Supplemental Table S4).

A

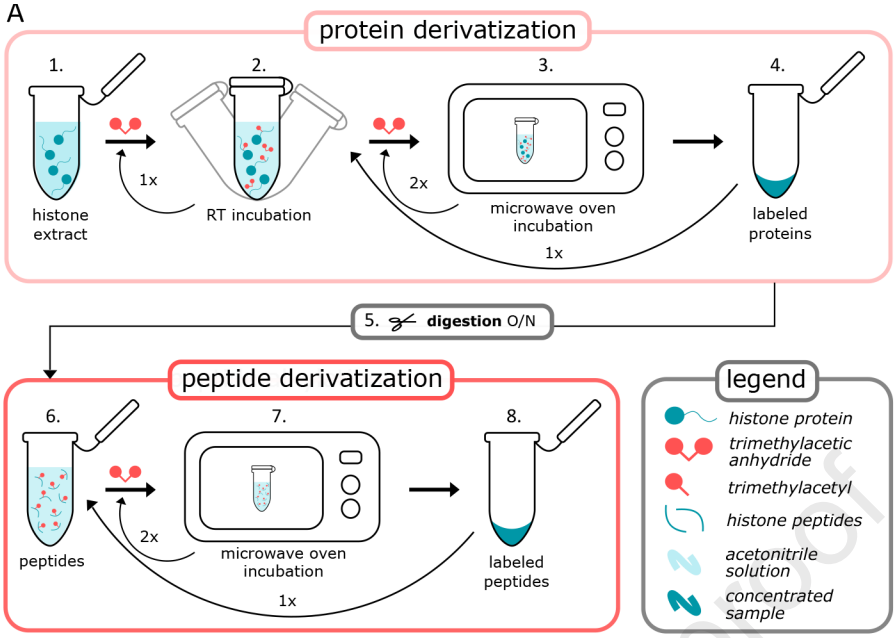

B

1. Dilute 12 µg of histone extract to a final concentration of 1 µg.µL^{-1} in 50% ACN (v/v).
2. Adjust pH to 8 with NH_4OH, add 3 µL of derivatization reagent*, incubate in a thermomixer (1000 rpm) at RT for 5 h. Then repeat this step with 16 h incubation. Reduce sample volume in a vacuum concentrator to 5 µL.
3. Dilute sample with 50% ACN to a final concentration of 1 µg.µL^{-1} and perform 3 sub-cycles of derivatization in microwave oven; for each cycle: adjust pH to 8 with NH_4OH, add 3 ul of derivatization reagent*, incubate in a microwave oven (350 W, 2x 1 min – with spin between incubations).
4. Reduce sample volume in a vacuum concentrator to 5 µL, and repeat step 3.
5. Reduce sample volume in a vacuum concentrator to 5 µL, dilute with 40 µL of 100 mM ABC. Perform two subsequent trypsin digestion (E:S=1:40, w/w) at 37°C for 4 h and 12 h. Reduce sample volume in a vacuum concentrator to 5 µL.
6. Dilute sample with 50% ACN to a final concentration of 0.6 µg.µL^{-1} and perform 3 sub-cycles of derivatization in microwave oven; for each cycle: adjust pH to 8 with NH_4OH, add 3 µL of derivatization reagent*, incubate in a microwave oven (350 W, 2x 1 min – with spin between incubations).
7. Reduce sample volume in a vacuum concentrator to 5 µL, and repeat step 6.
8. Dry sample in a vacuum concentrator.

* Derivatization reagent: mixture of ACN and TMA (v/v=3:1), freshly prepared

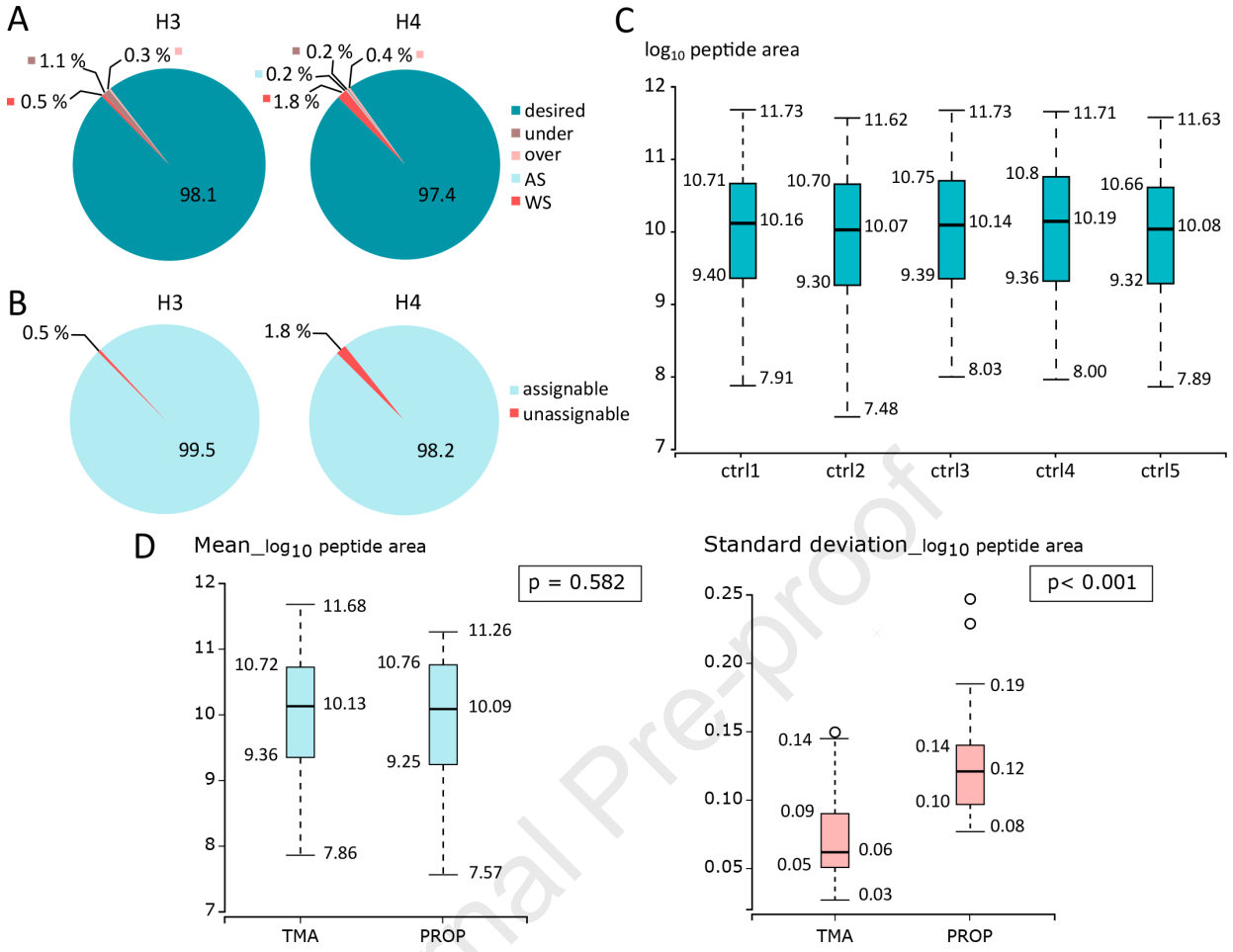

A

	K5K8K12K16	TMA	Prop
0 Ac	no modification	✓	✓
1 Ac	K5ac	✓	X
	K8ac	✓	co-elution
	K12ac	✓	
	K16ac	✓	✓
2 Ac	K5acK8ac	co-elution	X
	K5acK12ac		✓
	K5acK16ac	✓	X
	K8acK12ac	✓	X
	K8acK16ac	✓	co-elution
	K12acK16ac	✓	
3 Ac	K5acK8acK12ac	✓	co-elution
	K5acK12acK16ac	co-elution	
	K5acK8acK16ac		X
	K8acK12acK16ac	✓	X
4 Ac	K5acK8acK12acK16ac	✓	✓

B

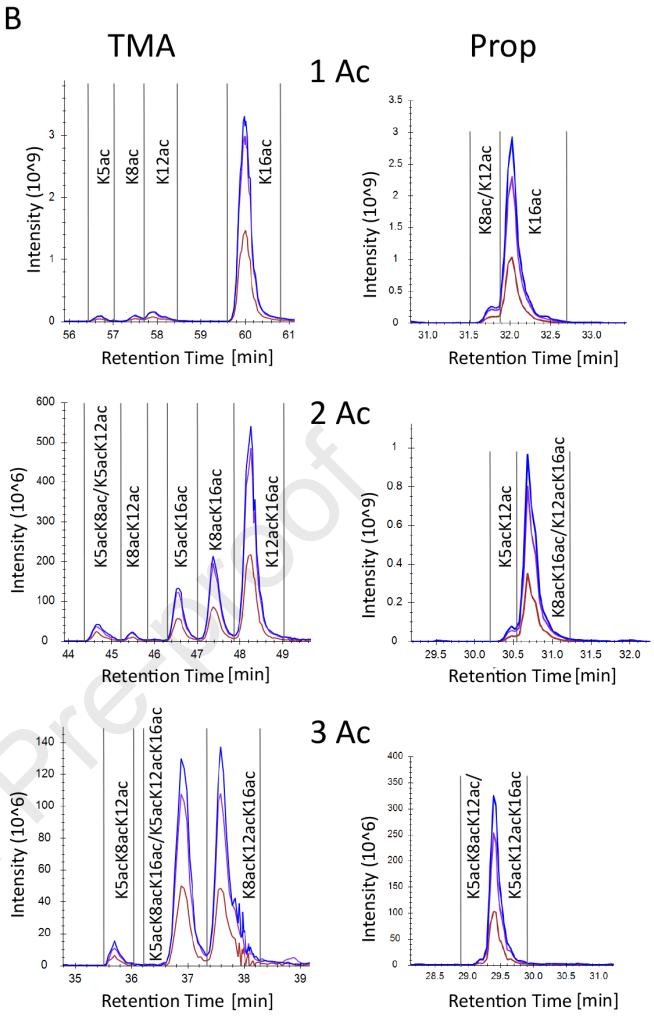

C

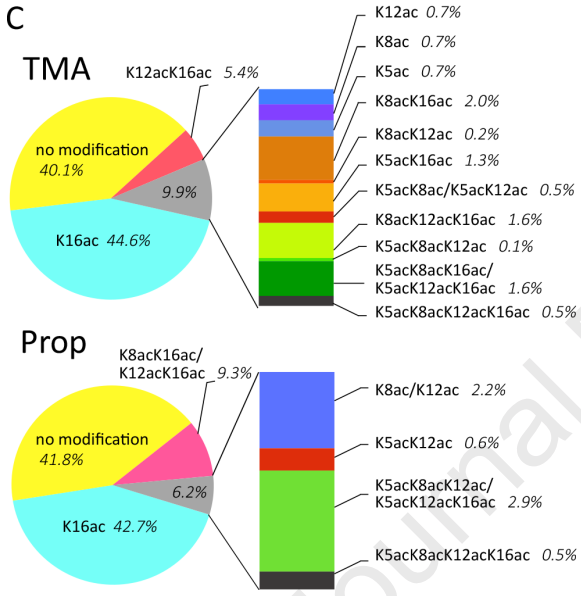

A

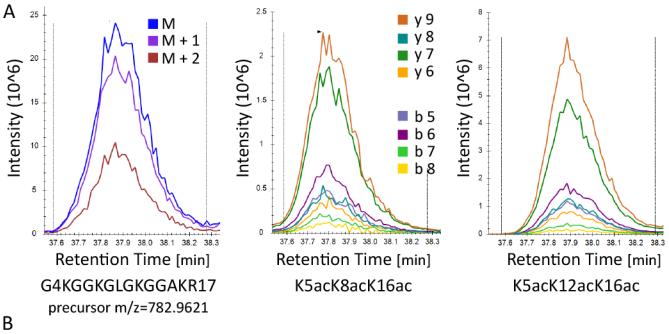

B

Sequence		K5acK8acK16ac	K5acK12acK16ac		K5acK8acK16ac	K5acK12acK16ac
G				b1	142.086	142.086
K	y13	1423.838	1423.838	b2	312.192	312.192
G	y12	1253.732	1253.732	b3	369.213	369.213
G	y11	1196.711	1196.711	b4	426.235	426.235
K	y10	1139.690	1139.690	**b5**	**596.340**	**638.387**
G	**y9**	**969.584**	**927.537**	**b6**	**653.362**	**695.409**
L	**y8**	**912.563**	**870.516**	**b7**	**766.446**	**808.493**
G	**y7**	**799.478**	**757.432**	**b8**	**823.467**	**865.514**
K	**y6**	**742.457**	**700.410**	b9	1035.620	1035.620
G	y5	530.305	530.305	b10	1092.641	1092.641
G	y4	473.283	473.283	b11	1149.663	1149.663
A	y3	416.262	416.262	b12	1220.700	1220.700
K	y2	345.224	345.224	b13	1390.805	1390.805
R	y1	175.119	175.119			

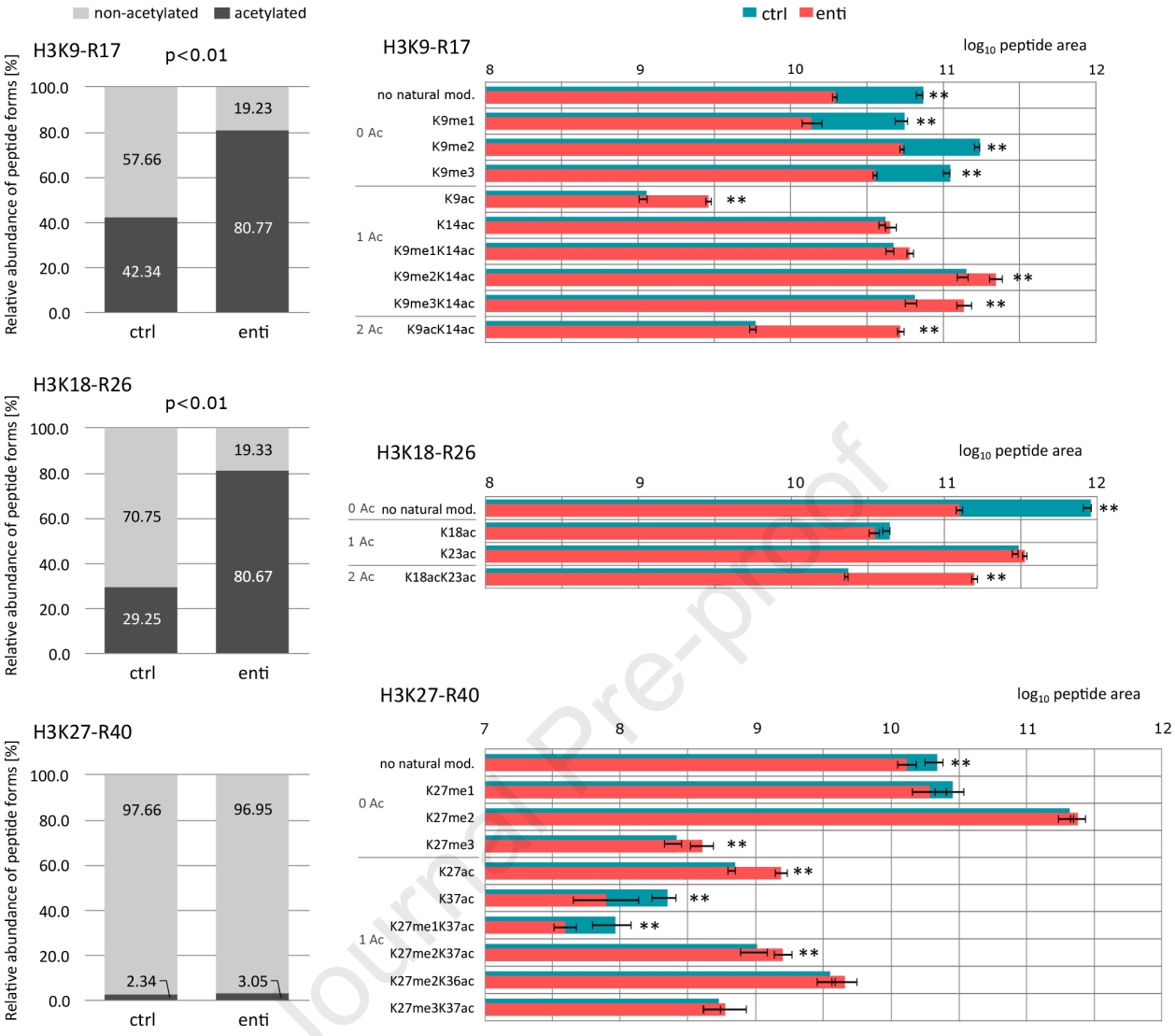

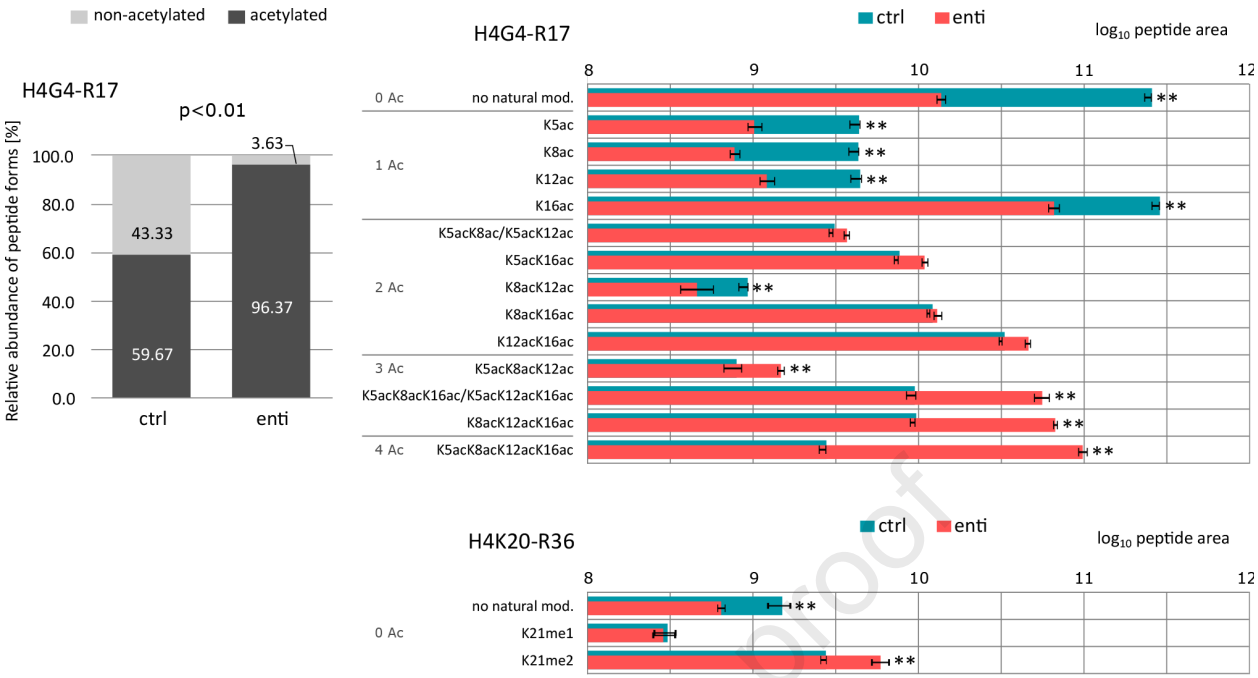

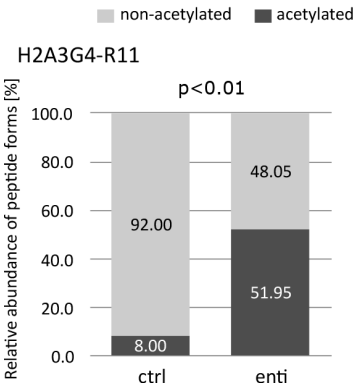

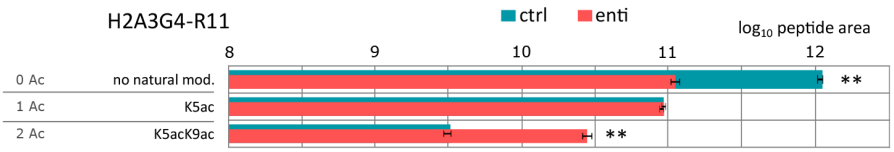

Trimethylacetic anhydride-based derivatization facilitates quantification of histone marks at the MS1 level

Authors

Hana Kuchaříková, Pavlína Dobrovolná, Gabriela Lochmanová, Zbyněk Zdráhal

Highlights

- Microwave-assisted labelling of histones using TMA for bottom-up proteomics
- TMA enables discrimination of isobaric peptides by improved chromatographic behaviour
- TMA facilitates histone quantification from MS1-level spectral information
- TMA provides excellent overall performance for monitoring hPTM pattern in the tissues

Trimethylacetic anhydride-based derivatization facilitates quantification of histone marks at the MS1 level

Authors

Hana Kuchaříková, Pavlína Dobrovolná, Gabriela Lochmanová, Zbyněk Zdráhal

In Briefs

The discrimination of isobaric peptides represents a common challenge in histone characterization. This study reports trimethylacetic anhydride (TMA) as a novel derivatization reagent for bottom up proteomics of histone proteoforms. TMA substantially improves separation of positional isomers which is a prerequisite for identification and quantification of post-translationally modified histone forms.

Brno, May 7th, 2021

All co-authors have contributed to manuscript and have seen and agree with the contents of the manuscript. The authors declare no financial interest to report. We certify that the submission is original work, has not been previously published and has not been submitted for publication elsewhere while under consideration.

Gabriela Lochmanová on behalf of the authors.

CEITEC – Central European Institute of Technology

Masaryk University

Kamenice 753/5, 625 00 Brno, Czech Republic

www.ceitec.eu